OPTOELECTRONICS AND ADVANCED MATERIALS – RAPID COMMUNICATIONS Vol. 3, No. 5, May 2009, p. 472 - 476

Structural and optical characterization of dip coated PbS nano-structured films prepared at different reaction temperatures

M. ABDEL RAFEA*, N. ROUSHDY
Electronic Materials Dep., Advanced Technologies and New Materials Institute
Mubarak City for Scientific Research and Technology Applications P.O. Box 21934 New Borg El-Arab, Alexandria, Egypt

PbS thin films were deposited by dip coating technique from lead acetate and thiourea in the reaction temperature range 100-200 °C. Nano structured PbS cubic phase was identified by XRD. Crystallite size of 4.8 nm was observed at lower reaction temperature and increased to 5.5 nm as the reaction temperature increases or by annealing at the same reaction temperature. Nano grains in the range 30-70 nm was observed by SEM. EDX analysis shows that the films composition are close to stiochiometric value for all deposited films. Optical absorption and dispersion were deduced from the transmittance curve only for films deposited with different thicknesses. Mathematical treatment was applied to calculate the optical parameters α, E_g, n and K. The absorption edge was shifted towards the visible region due to band gap increase due to strong confinement effect in nano structured system.

(Received May 19, 2009; accepted May 25, 2009)

Keywords: PbS, nanostructured films, Dip coating, Structural and optical properties

1. Introduction

Narrow band gap lead sulfide of 0.41 eV at room temperature is commonly used in infrared detectors due to high photo-sensitivity to infrared region [1]. The optical absorption edge can be shifted from infrared to visible region by energy gap confinement effect due to large exciton Bohr radius (18 nm) [2]. Different structures of PbS have been prepared[3-10]. Several attempt to shift the absorption edge of PbS to the visible region to be used as solar absorber layer such a partial substitution of lead by antimony [11] or by shift the absorption edge to longer wavelengths for far infrared detectors by partial substitution of the sulfur by selenium [12]. PbS nanopowder a well as many metals sulfides such as Zn and Mn were prepared by reaction of those metal acetate with thiourea at 185 °C for three h in air [13] the reaction procedure was explained as the thiourea is in the melt state and behaves just as a liquid reactant, which can enormously increase the interfaces and contact surface areas with the other solid reactants. In this work we have proven that PbS can be prepared at temperature lower than the melting point of thiourea (185 °C). Besides, simple dip coating of the same starting materials can produce nanostructured film instead of powder, which is more applicable in application.

2. Experimental

5N lead acetate, thiourea were used to prepare PbS thin films. 0.1 M of lead acetate was dissolved in 100 ml Ethanol, stirred for 10 min. An equivalent molar concentration of thiourea was added to the solution and stirred for another 10 min., then ultrasonically homogenized then wormed with stirring for 10 min until a colorless and clear solution was obtained. The precursor was used directly for dip coating technique on pre-cleaned glass substrates. Glass slides of dimension 20x70x2 mm were cleaned by using ultrasonic cleaner, detergent, HCl, double distilled water and finally rinsing with ethanol, respectively Pre-cleaned and optically flat glass slides were dipped in the solution, then pulled out slowly, vertically and dried in air. Films of the starting materials are nearly homogeneous at the two glass sides; one of them was erased using cotton and ethyl. The film heated in the muffle at the reaction temperatures 100 °C for 10 min. Dark brownish film was observed after heating. After the film was cooled down to room temperature, another dip coating process was done again in order to deposited another layer. A set of one sided layers were deposited until 8 layers with high transparency and uniformity. Other set of films were prepared under the same preparation conditions but the reaction temperatures were increase to be 120, 140, 160, 180 and 200 °C in order to study at which temperature the PbS phase is formed. The crystalline structure was measured and identified using Shimadzu XRD 7000 maxima powder diffraction at the conditions; tube voltage 30 KV, current 30 mA and wavelength $CuK_{\alpha 1}$, λ=1.5406 Å using Ni filter. The scan range was 2θ=10-100° and scan speed was 1°/min. SEM of type Jeol-JSM-636 OLA was used to study the surface morphology of the prepared powder and the deposited films. The film thickness was determined by the cross sectional imaging of the film and the substrate broken edge. The composition of the powder and films were determined using the energy dispersive x-ray spectroscopy technique attached with the scanning electron microscope.

The optical transmittance was measured for the films using double beams UV-VIS spectrophotometer type LABOMED of spectral range 190-1100 nm with a scan step of 2 nm using reference glass substrate.

3. Results and discussion

3.1 Crystalline structure

X-ray diffraction patterns of the as PbS thin films at different reaction temperatures are shown in Fig.(1). Polycrystalline Pbs are the main features of the films. Two characteristic XRD peaks were identified using ICDDVIEW 2006 data base, card ID 00-001- 0880. The peak of the highest intensity in the standard card (powder) is *hkl* (111), while in the film a preferred orientation at (200) during the growth process took place. Fewer peaks in the films were detected than in the powder. Broadening of the diffracted peaks was used to determine the average crystallite size (D) using Scherrer equation

$$D = \frac{0.95\lambda}{\beta \cos\theta} \text{ and } \beta = \sqrt{\beta^2_{sample} - \beta^2_{silicon}} \qquad (1)$$

β_{sample} and $\beta_{silicon}$ are the full widths at half maxima (FWHM) of the broadened peaks of the sample and a silicon crystal free from defects, respectively.

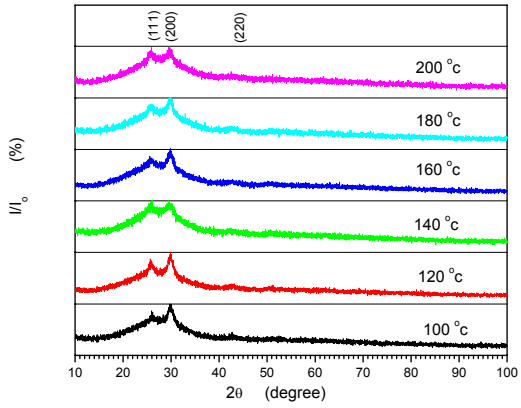

Fig.1. XRD of the as deposited PbS thin films.

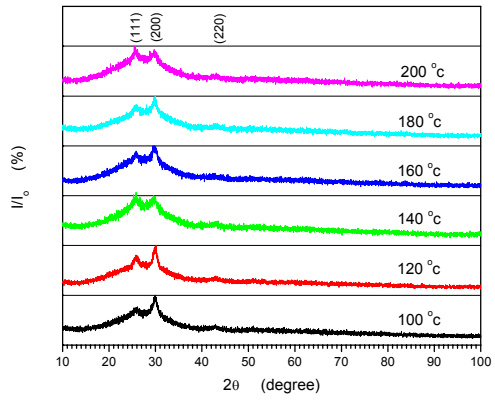

Fig. 2. XRD of PbS annealed thin films for 1h.

The use of silicon crystal free from defects enables to determine the instrumental broadening. The average crystallite size was found to be 4.8 nm with variance 0.4 nm in the whole temperature range 100-200 °C. Annealing of the films at the same reaction temperature for one h increases the crystallite size to 5.5 nm and varied about 0.3 nm in the whole temperature range. Fig. 2 shows the diffraction patterns of PbS annealed films. It was observed that the preferred orientation changed from the (200) peak to (111) peak for film deposited at 200 °C.

3.2 Surface morphologies

The surface morphology of the PbS films is shown in Fig. 3 as a representative image. Generally, the films microstructure consists of fine grains of sizes in the in the range 30-70 nm. Some bigger grains consists of smaller grains that agglomerates. The cross sectional image resolve the film boundaries which determines the films thickness. The average films thickness was found to be 497±5nm as shown in Fig. 4. The elemental analysis of the films were measured using EDX is represented in Fig.(5). The calculated atomic percentages are 50.67 and 49.33 % for S and Pb, respectively.

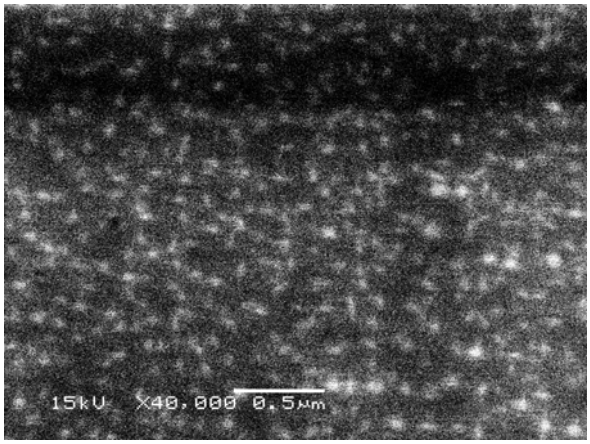

Fig. 3. SEM of PbS film deposited at 200 °C.

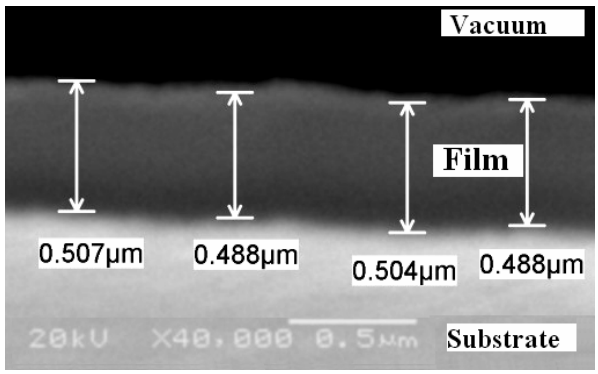

Fig. 4. Thickness measurement from Cross sectional image.

3.3 Optical properties

3.3.1 Absorption

A representative curve of optical transmittances for PbS thin film films prepared at 140 ^{o}C is shown in Fig. 6. Dark brown color films with transmittance 40-50 % in the longer wavelength region.

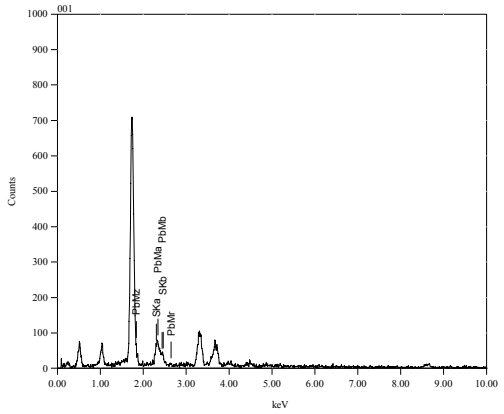

Fig.5. EDX analysis of PbS thin films [Pb:S=49.33 : 50.67].

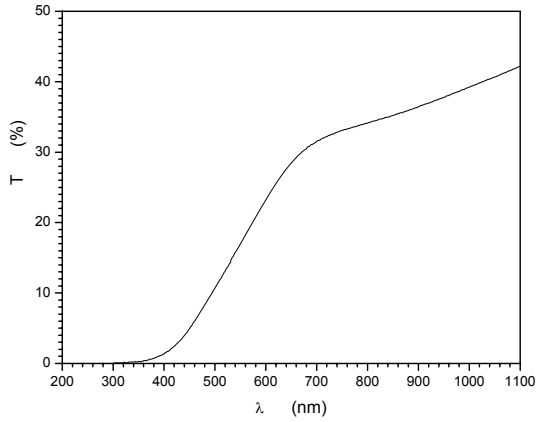

Fig. 6. T as representative curve of PbS thin film prepared at 140 ^{o}C.

Because of Pb chalcogenides possesses high refractive index, the reflection becomes higher. We deduce a mathematical method to eliminate the the reflection factor which was not measured in our spectrophotometer. Films of different thicknesses were measured at the same preparation conditions in order to determine the absorption coefficient as follows:

The relationship between the optical transmittance (T), the absorption coefficient (α), thickness, (d), and reflectance (R) is given by the relation [14, 15]:

$$T = (1-R)^2 .e^{-\alpha d} \qquad (2)$$

Using the smaller film thickness of transmittance T_1 and thickness d_1

$$T_1 = (1-R)^2 .e^{-\alpha d_1} \qquad (3)$$

Dividing Eqn.(2) by Eqn.(3) and deduce the absorption coefficient, the reflectance (R) will be eliminated, we get:

$$\alpha = -\frac{1}{d-d_1}.\ln\left(\frac{T}{T_1}\right) \qquad (4)$$

Eqn.(4) was used to calculate the absorption coefficient for the other thicker films. PbS is direct band gap semiconductor the absorption coefficient follows the relation:

$$\alpha = \beta \frac{\sqrt{h\nu - E_g}}{h\nu} \qquad (5)$$

where β is constant and E_g is the band gap. In order to determine the band gap a plot of $(\alpha h\upsilon)^2$ Vs hυ produces a straight lines of intercept with the photon energy axis at E_g. The method was applied for all films, Fig. 7 and Fig. 8 show $(\alpha h\upsilon)^2$ Vs hυ for the as deposited and annealed films. It was observed that a slight change in the band gap with changing the reaction and annealing temperatures while the band gap itself is more higher than in literature (0.41 eV) [1,2].

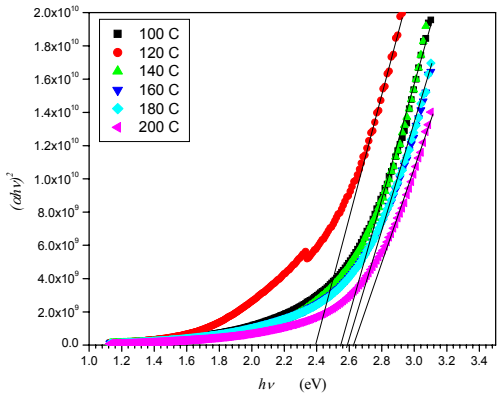

Fig. 7. $(\alpha h\nu)^2$ vs. $h\nu$ for PbS as deposited thin films.

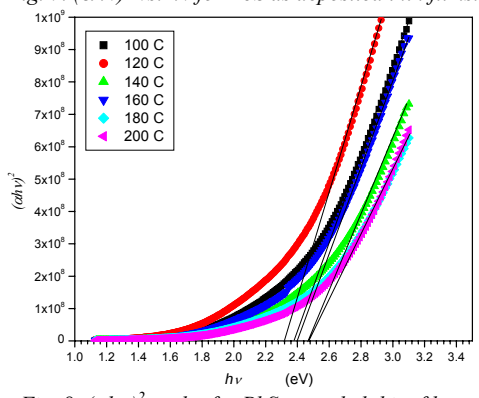

Fig. 8. $(\alpha h\nu)^2$ vs. $h\nu$ for PbS annealed thin films.

In our study, the band gap are in the range 2.4-2.6 eV for the as deposited films and 2.3-2.5 eV for the annealed ones. This large shift of band gap can be explained by the strong energy gap confinement phenomena that the crystallite size (4-5 nm) is much smaller than the exciton radius (18 nm). This phenomena was discussed by many workers in low excitonic radius materials and in previous works in chalcogenides and oxides semiconducting materials such as oxides [16] and chalcogenides [17,18]. The relation between the band gap of nanostructured materials and crystallite size can be expressed in the frame of Brus Model [19]

$$E_g(D) = E_{g.Bulk} + \frac{h^2}{8m_o D^2}\mu - \frac{1.8e^2}{4\pi\varepsilon_o\varepsilon_r D} - \frac{0.248\times 4\pi^2 e^4 m_o}{2h^2(4\pi\varepsilon_o\varepsilon_r)\mu} \quad (6)$$

where μ is the effective mass. The term $(h^2\mu/8m_oD^2)$ is the quantum localization (*i.e.* the kinetic energy term). It obviously shifts E_g(D) to higher energies. The term $(-1.8e^2/4\pi\varepsilon_o\varepsilon_r D)$ is due to the screened Coulomb interaction between the electron and the hole, it shifts $E_g(D)$ to lower energies. The last term is size independent due to spatial correlation effects and is usually small in both the value and the effect on E_g(D) [20-23]. As the crystallite size decreases the quantum localization term is predominant the band gap shift to higher energies which our case. By this interesting phenomenon the absorption edge can be displaced to higher photon energy (from IR 0.4 to UV 2.5 eV).

3.3.2 Dispersion

Optical transmission measurements of two films with different thicknesses enable to determine the absorption coefficient as explained above. Reflectance can be estimated from the measured absorption coefficient, α, in Eqn. 1 or 2. the reflectance is then given by:

$$R = 1 - \sqrt{Te^{\alpha d}} \quad (7)$$

The relation between the optical reflectance, refractive index and extinction coefficient is governed by the following relation [24].

$$R = \frac{(n-1)^2 + K^2}{(n+1)^2 + K^2}, \qquad K = \frac{\alpha\lambda}{4\pi} \quad (8)$$

Eqn(8) can be solved in n by the following relation:

$$n = 1 + \sqrt{\frac{4(2-R)}{(1-R)} - K^2} \quad (9)$$

Applying Eqn.(7), Eqn.(8) and Eqn.(9) to α and T in order to calculate both n and K. The calculated refractive index for the as deposited and annealed films are represented in Fig. 9 and Fig. 10. The refractive index shows nearly constant value at the longer wavelength which is in the range 6.09-4.85, while an increase was observed near the absorption edge due to dispersion phenomena.

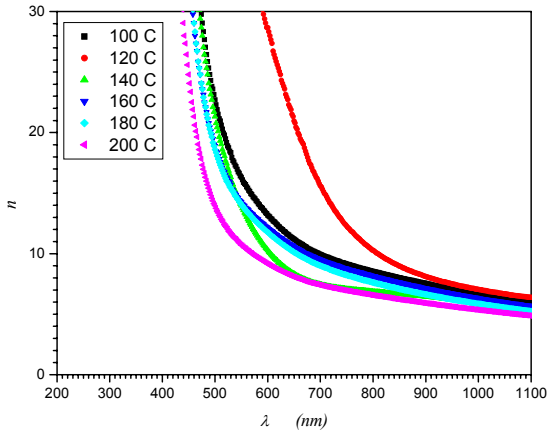

Fig. 9. Refractive index of PbS as deposited films.

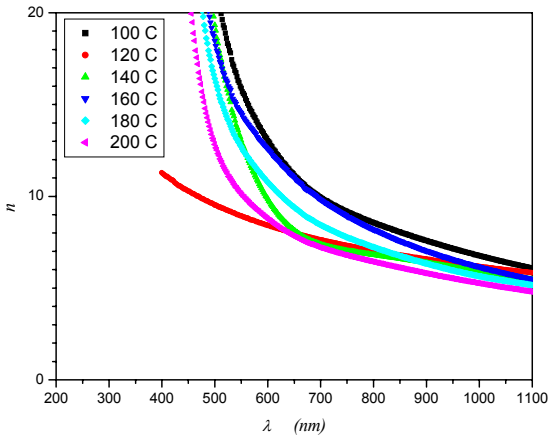

Fig. 10. Refractive index of PbS annealed films.

The average value of refractive index at longer wavelengths of the as deposited and annealed films at 100 ^oC was found to be 6.09 which decreases linearly to 4.85 as the reaction and annealing temperature increases to 200 ^oC. Fig. 11 and Fig. 12 show the extinction coefficient of the as deposited and annealed films.

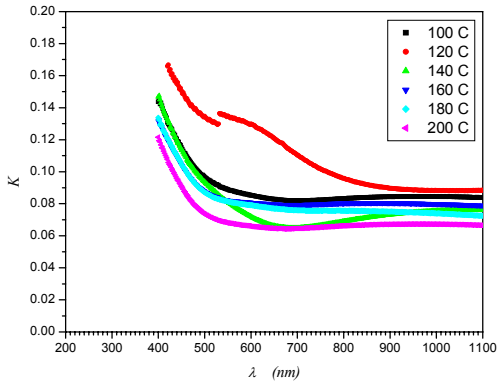

Fig. 11. Extinction coefficient of PbS as deposited films.

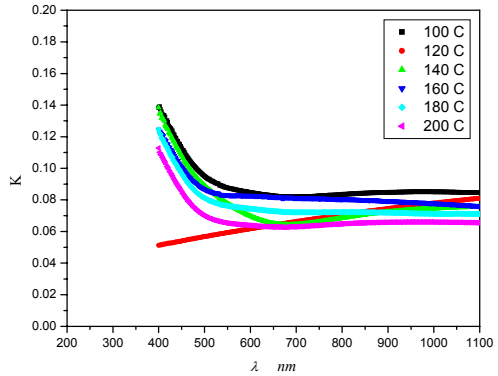

Fig. 12. Extinction coefficient of annealed PbS films.

Because of strong relationship between the absorption coefficient and extinction coefficient they behave as similar manner: minimum absorption at long wavelengths below the absorption edge, while absorption process took place around the wavelength range that corresponds to the band gap.

4. Conclusions

Nanostructured PbS films have been deposited by simple dip coating technique. Nanocrystallites of diameter range 4.8-5.5 nm were calculated from XRD peak profiles while nanograins at the film surface of size 30-70 nm was observed by SEM. EDX analysis shows that the films are stiochiometric. Optical absorption and dispersion was deduced from the transmittance curve only. Mathematical treatment was done to calculate the optical parameters α, E_g, n and K. The absorption edge was shifted towards the visible region due to band gap increment. The band gap increases due to strong confinement effect of the nanostructured PbS film because of low effective mass and larger excitonic radius of PbS.

Acknowledgments

This work was carried out through the support from the Mubarak City for Scientific Research and Technology Applications (MUCSAT), research program of the Institute of Advanced Technologies and New materials.

References

[1] E. Pentia, L. Pintilie, I. Matei, T. Botila, I. Pintilie, Infrared Physics & Technology **44**, 207 (2003).
[2] S. Jana, R. Thapa, R. Maity, K. K. Chattopadhyay, Physica E **40**, 3121 (2008).
[3] D. Liang, S. Tang, J. Liu, J. Liu, X. Lv, L. Kang, Materials Letters **62**, 2426 (2008).
[4] R. S. Patil, C. D. Lokhande, R. S. Mane, T. P. Gujar, S.-H. Han, J. Non-Crystalline Solids **353**, 1645 (2007).
[5] M. Orphanou, E. Leontidis, T. Kyprianidou-Leodidou, W. Caseri, F. Krumeich, K. C. Kyriacou, J. Colloid and Interface Science **302**, 170 (2006).
[6] Z. Xiu, S. Liu, J. Yu, F. Xu, W. Yu, G. Feng, J. Alloys and Compounds **457**, L9 (2008).
[7] K. P. Fritz, S. Guenes, J. Luthe, S. Kumar, N. S. Sariciftci, G. D. Scholes, J. Photochemistry and Photobiology A: Chemistry **195**, 39 (2008).
[8] M. Wu, H. Zhong, Z. Jiao, Z. Li, Y. Sun, Colloids and Surfaces A: Physicochem. Eng. Aspects **313–314,** 35 (2008).
[9] T. Duan, W. Loua, X. Wang, Q. Xue, Colloids and Surfaces A: Physicochem. Eng. Aspects **310,** 86 (2007).
[10] X.-L. Zhao, C.-X. Wang, X.-P. Hao, J.-X. Yang, Y.-Z. Wu, Y.-P. Tian, X.-T. Tao, M.-H. Jiang, Materials Letters **61**, 4791 (2007).
[11] M. Y. Versavel, J. A. Haber, Thin Solid Films **515**, 5767 (2007)
[12] S. Kumar, M. A. Majeed Khan, S. A. Khan, M. Husain, Optical Materials **25**, 25 (2004).
[13] Z. Y. Xu, Y. Cai Zhang, Materials Chemistry and Physics **112**, 333 (2008).
[14] R. Sahraei, G. M. Aval, Al. Goudarzi, J. Alloys and Compounds **466**, 488 (2008).
[15] J. C. Manifacier, J. Gasiot, J. P. Fillard, J. Phys.E: Sci. Instum. **9**, 1002 (1976).
[16] El-Sayed M. Farag, Optics & Laser Technology **36,** 35 (2004).
[17] M. Abdel Rafea, N. Roushdy, J. Phys. D: Appl. Phys. **42,** 015413 (2009).
[18] M. Abdel Rafea, J. Mater Sci: Mater Electron **18**, 415 (2007).
[19] M. Abdel Rafea, H. Farid, Materials Chemistry and Physics **113**, 868 (2009).
[20] B. Pejova, A. Tanusevski, I. Grozdanov, J. Solid State Chem. **177**, 4785 (2004).
[21] H. Hao, X. Yao, M. Wang, Optical Materials **29**, 573 (2007).
[22] B. Pejova, I. Grozdanov, Materials Letters **58**, 666 (2004).
[23] B. Pejova, I. Grozdanov, Materials Chemistry and Physics **90**, 35 (2005).
[24] A. Abu EL-Fadl, Galal A. Mohamad, A.B. Abd El-Moiz, M. Rashad, Physica B **366**, 44 (2005).

*Corresponding author: m.abdelrafea@mucsat.sci.eg